

Final Project Report

Determination of the Curing Efficiency of Externally and Internally Cured Concrete Using Neutron Radiography

Concrete Research Council (CRC), ACI Foundation

CRC 2020 P0036

Mehdi Khanzadeh Moradllo, Lynda Bouchelil, Gwen Clark

Temple University

Philadelphia, Pennsylvania

W. Jason Weiss, Rita Maria Ghantous, Margaret N. Goodwin

Oregon State University

Corvallis, Oregon

December 2021

**Concrete Research Council (CRC), ACI Foundation
FINAL REPORT**

Lead Organization: Temple University

| | | |
|--|--|--|
| ACI Foundation Project # <i>CRC 2020 P0036</i> | | Report Period: July 2020 – December 2021 |
| Project Title: Determination of the Curing Efficiency of Externally and Internally Cured Concrete Using Neutron Radiography | | |
| Name of PI/Co-PI: Mehdi Khanzadeh Moradllo (TU) W. Jason Weiss (OSU) | Phone Number: 215-204-6164 541-737-1885 | E-Mail Mehdi.khanzadeh@temple.edu Jason.weiss@oregonstate.edu |
| Project Start Date: July 01, 2020 | Project End Date: December 20, 2021 | Number of Extensions: 0 |

Project Advisory Committee Members:

Kenneth Hover, Professor – Cornell University
Jeffrey Speck, Past Chair – ACI 213
Bill Wolfe, Member – ACI 213
Larry Taber, Past Chair – ACI 308
Oscar Antommattei, Member – ACI 308

ACI Foundation Staff:

Ann Masek, Executive Director
Tricia Ladely, Assistant Director

Project Executive Summary

Curing is important to develop long-lasting durable concrete. Curing promotes hydration of the cement and reaction of the supplementary cementitious materials (SCMs) leading to improved strength and durability. Concrete specifications typically specify curing as a fixed duration of time (e.g., 14 days of curing using wet burlap). Currently, State Highway Agencies (SHA) are actively seeking ways in which they can reduce the time of construction to reduce the inconvenience to the traveling public and to improve safety for the construction workers in work zones. As such, it is often asked if the specified duration of curing can be reduced, especially by implementing new curing practices. However, relatively limited work has been performed to understand how the benefits of new curing practices (e.g., internal curing) can be achieved in the construction process. This study proposes a new methodology to quantify the effectiveness of external and internal curing with high spatial resolution over concrete depth. This research develops quantifiable equivalent durations of curing for concrete with conventional curing and internal curing, especially in SCM systems. It is shown that the use of internally cured concrete mixtures can reduce curing time, saving contractors both time and money during construction. For example, while a 14-day wet burlap may be specified on a bridge deck, it may be possible that 7 days of wet burlap with internal curing provides the same level of performance. This would reduce the construction schedule by one week.

The immediate findings of this study will provide tools to enable practitioners to implement internal curing for different applications due to its advantages in saving both time and money during construction. It also helps to evaluate the performance of different external curing methods by quantifying the depth of the curing-affected zone with high spatial resolution. In addition, the outcomes of this research can be directly incorporated into a new ACI guide to internal curing (ACI 308-213R).

The objectives of this study are:

- Develop a new methodology to evaluate curing efficiency in concrete mixtures with and without SCMs. This method can quantify the influence of external and internal curing on the degree of hydration of cementitious systems with high spatial resolution.
- Examine the impact of internally cured concrete on the duration of curing determine equivalent performance to conventional externally cured concrete.
- Establish new curing guidelines for SCM and internally cured systems.

Acknowledgments

The authors gratefully acknowledge the financial support for this study by American Concrete Institute (ACI) Foundation and Temple University. The authors gratefully acknowledge support from the Edwards Distinguished Chair at Oregon State University, which has supported Professor W. Jason Weiss. The authors would like to acknowledge the OSU Radiation Center's operation team for their assistance with conducting the neutron radiography experiment. The invaluable support of the project advisory team is much appreciated. We are also thankful to Lehigh Cement, JDM Materials, Northeast Solite Corporation, Ferroglobe, WR Meadows, and GCP Applied Technologies for donating materials.

Disclaimer

The contents of this report reflect the views of the authors who are responsible for the facts and accuracy of the data presented herein. The contents do not necessarily reflect the official views of the funding organizations at the time of publication. This report does not constitute a standard, specification or regulation.

Table of Contents

| | |
|--|----|
| 1. Introduction..... | 1 |
| 2. Materials and Methods..... | 3 |
| 2.1 Materials | 3 |
| 2.2. Mixture proportions | 4 |
| 2.3. Curing and conditioning | 4 |
| 2.4. Neutron Radiography (NR) | 6 |
| 2.5. Determining the non-evaporable water profiles using NR..... | 7 |
| 2.6. Thermogravimetric analysis (TGA)..... | 8 |
| 3. Results and Discussion | 9 |
| 3.1. Non-evaporable water profiles..... | 9 |
| 3.2. Determining the curing-affected zone (CAZ) as a function of curing time | 14 |
| 3.3. Establishing ‘Equivalency Lines’ | 17 |
| 3.4. Practical implications | 19 |
| 4. Conclusions..... | 20 |
| 5. References..... | 21 |
| Appendix: TechNote Outline | 25 |

List of Tables

Table 1 – Chemical compositions and physical properties of cementitious materials from XRF.

Table 2 – Mixture proportions (saturated surface dry condition).

Table 3 – External curing practices.

Table 4 – Specifications of the curing compounds used.

List of Figures

Figure 1 – Schematic representation of (a) wet burlap curing, (b) drying process (conditioning), and (c) preparation of the mortar samples for NR testing.

Figure 2 – NR experimental set up: (a) plan view of NRF at OSU (adapted from <https://radiationcenter.oregonstate.edu/oregon-state-triga-reactor-0>) (b) an example of NR image obtained from mortar sample, and (c) an example of analyzed results ($V_{Non-evaporable\ water}$ over depth).

Figure 3 – Profiles of volume fraction of non-evaporable water over depth for OPC and FA mortar samples ($w/cm=0.45$) with varying wet burlap curing durations: (a) P-0.45, (b) PIC-0.45, (c) FA-0.45, and (d) FAIC-0.45.

Figure 4 – Profiles of volume fraction of non-evaporable water over depth for OPC and SF mortar samples ($w/cm=0.35$) with varying wet burlap curing durations: (a) P-0.35, (b) PIC-0.35, (c) SF-0.35, and (d) SFIC-0.35.

Figure 5 – The $V_{Non-evaporable\ water}$ in the core of the samples (40-60 mm from the exposed surface) as a function of wet burlap curing time for different mortar mixtures with and without IC (by TGA): (a) OPC- $w/cm=0.45$, (b) FA- $w/cm=0.45$, (c) OPC- $w/cm=0.35$, and (d) SF- $w/cm=0.35$.

Figure 6 – Comparison between $V_{Non-evaporable\ water}$ profiles for FA mortar samples ($w/cm=0.45$) with CC-Resin and CC-PAMs curing compounds and 1-day and 7-day wet burlap cured samples: (a) FA-0.45 and (b) FAIC-0.45.

Figure 7 – Determination of the CAZ using the non-evaporable water profile by NR.

Figure 8 – CAZ as a function of wet burlap curing time for different mortar mixtures with and without IC: (a) OPC- $w/cm=0.45$, (b) FA- $w/cm=0.45$, (c) OPC- $w/cm=0.35$, and (d) SF- $w/cm=0.35$.

Figure 9 – Comparison of CAZ for FA samples ($w/cm=0.45$) with curing compound and wet burlap curing methods.

Figure 10 – (a) Determination of equivalent points between the virgin and IC mixtures using CAZ profiles (difference between the fitted curves) and (b) an example of the correlation between the use of IC and equivalent external curing durations (i.e., equivalency line using CAZ).

Figure 11 – Correlation between the use of IC and equivalent external curing durations (i.e., equivalency line using CAZ): (a) OPC and FA mixtures ($w/cm=0.45$) and (b) OPC and SF mixtures ($w/cm=0.35$).

1. Introduction

Curing is important to develop strong and durable concrete.¹ Curing promotes the hydration of the cement and reaction of the supplementary cementitious materials (SCMs).¹⁻³ Curing primarily consists of external water supplied through wet fabrics (e.g., burlap) or application of external sealing membranes such as curing compounds to minimize water loss from the concrete.^{1, 3-5} Internal curing (IC) provides a supplemental method of curing concrete. IC typically consists of partially replacing the fine aggregates with an equivalent volume of pre-wetted fine lightweight aggregates (FLWA) or superabsorbent polymers (SAPs). The FLWA or SAP serves as the internal water reservoirs for curing.⁶⁻¹¹

Internal curing improves bridge deck concrete by reducing early-age cracking, which enhances the durability and sustainability of concrete infrastructure.^{6, 12-13} IC also has been used to reduce cracking in high-early-strength (HES) patches.^{6, 11} A guide specification was developed to help the State Highway Agencies (SHA) to implement internally-cured concrete for field applications.^{8, 11-14} While substantial work has been performed on IC concrete,⁶⁻¹² a relatively limited amount of this work has focused on how IC impacts the construction processes. Most notably, limited work has been performed to evaluate whether reductions in the duration of external curing are possible when IC is used.⁶ If IC can result in reduced external curing time, this may provide the SHA with a tool to reduce the time of construction, inconvenience to the traveling public, and to improve safety for the construction workers in work zones.¹⁵

Several test methods have been implemented to examine curing efficiency by either measuring moisture/moisture loss or surface/near-surface physical properties.^{4, 16-22} Examples include the use of RH sensors near the surface of concrete and the bulk physical or transport property measurements such as permeability, water absorption, abrasion resistance, and hardness of the surface concrete.^{5, 17-19, 21-24} Recent research has demonstrated that curing efficiency can be quantitatively measured using neutron radiography (NR).²⁵ NR can quantitatively determine the extent of hydration reaction (i.e., the volume of chemically bound water) over the depth and the depth of the curing-affected zone (CAZ).^{25, 26} The CAZ is the thickness of concrete near the surface which can be impacted by external curing measures (i.e., the skin of the concrete, about 5-30 mm).^{16, 25, 26}

NR consists of exposing the sample to a neutron beam. In NR, a portion of the neutron beam passes through the concrete sample, and a portion of the beam is attenuated. The attenuation is primarily related to the neutron cross-section (a term used to express the likelihood that an incident neutron will interact with the target nucleus).²⁷ The neutron scattering and absorption cross-sections are particularly large for the first isotope of hydrogen,^{28,29} which makes this an ideal approach to study water content. As such, NR has been used to study the drying process, fluid absorption, plastic shrinkage, curing effectiveness, and cracking in cementitious materials.^{10, 25, 26, 30-38}

This study uses NR to quantify the effectiveness of external and internal curing by measuring non-evaporable water content (i.e., chemically bound water) over concrete depth in both Ordinary Portland Cement (OPC) and SCM systems. Non-evaporable water is chemically bound to the gel solids which are formed due to cement hydration or pozzolanic reaction of SCMs. This research quantifies the influence of different external and internal curing practices on the CAZ with a spatial resolution of about 90 micrometers. Equivalent curing durations for concrete made using conventional external curing and internal curing were determined. These equivalent performance criteria can be incorporated into curing guidelines and specifications. This would allow any benefits of using internally cured concrete to be quantified and used to reduce construction time and improve durability.

2. Materials and Methods

2.1 Materials

An ASTM C150 Type I ordinary portland cement was used in this study. Off-spec fly ash (FA) with a specific gravity of 2.78 and undensified silica fume (SF) with a specific gravity of 2.20 were implemented as supplementary cementitious materials (SCMs). The chemical compositions of cementitious materials are reported in Table 1. The fine aggregate is a natural river sand with a specific gravity of 2.63, and an absorption of 0.58%. Pre-wetted fine lightweight aggregates (FLWA) were used for internal curing (IC). The FLWA was an expanded shale, with a specific gravity of 1.85, and an absorption capacity of 18.5%. A polycarboxylate-based high range water reducer (HRWR) conforming to ASTM C494 (Type F) specification was used to achieve desirable slumps in low water-to-cementitious material ratio (w/cm) mixtures.

Table 1 – Chemical compositions and physical properties of cementitious materials from X-ray fluorescence (XRF).

| Component | Mass (%) | | |
|---------------------------------|----------|-------|-------|
| | OPC | FA | SF |
| SiO ₂ | 19.59 | 41.51 | 93.69 |
| Al ₂ O ₃ | 4.66 | 17.58 | - |
| Fe ₂ O ₃ | 2.78 | 6.34 | - |
| CaO | 63.30 | 24.09 | - |
| MgO | 3.45 | 4.79 | - |
| SO ₃ | 3.16 | 0.78 | 0.24 |
| Na ₂ O | 0.33 | 1.19 | - |
| K ₂ O | 0.95 | 0.48 | - |
| P ₂ O ₅ | - | 0.67 | - |
| Mn ₂ O ₃ | - | 0.04 | - |
| TiO ₂ | 0.22 | - | - |
| SrO | - | 0.33 | - |
| Na ₂ O _{eq} | 0.96 | 1.51 | 0.4 |
| LOI | 1.27 | 0.75 | 4.5 |

2.2. Mixture proportions

Eight mortar mixtures were prepared with two different w/cm (0.35 and 0.45) both with and without IC. The mixture proportions are provided in Table 2. The mortar mixtures contained 55% aggregate by volume. Pre-wetted FLWAs were used as the internal water reservoirs. FA and SF were used in mortar mixtures to replace 20% and 7.5% of the weight of cementitious materials, respectively (Table 2). The amount of FLWA for IC was chosen to provide a volume of water that was equivalent to the volume of chemical shrinkage developed by the cementitious materials, as described in ASTM C1761-15. The FLWA was oven-dried before being soaked in the total mixture water (mix water + IC water) for a period of 24 h before mixing. The mixtures were prepared following the ASTM C305-20 procedure. All the mortar mixtures were mixed in a planetary mixer with a capacity of 18.9 L (20 quarts). Prismatic samples (10.2 × 10.2 × 28.0 cm [4 × 4 × 11 inches], Figure 1) were cast to investigate the impact of different practices on curing efficiency by NR. After the mortar placement and consolidation, the mortar was screeded and finished to make a flat and smooth surface. Two samples per curing method were prepared.

Table 2 – Mixture proportions (saturated surface dry condition).

| Mixture | w/cm | Cement kg/m ³ (v*) | Fly ash kg/m ³ (v) | Silica fume kg/m ³ (v) | Sand kg/m ³ (v) | Water kg/m ³ (v) | FLWA kg/m ³ (v) | IC water kg/m ³ | WR % wt cm |
|-------------------|------|----------------------------------|----------------------------------|--------------------------------------|-------------------------------|--------------------------------|-------------------------------|-------------------------------|---------------|
| P-0.45 | 0.45 | 586.4 (0.19) | - | - | 1446.5 (0.55) | 263.9 (0.26) | - | - | - |
| P-IC-0.45 | | 586.4 (0.19) | - | - | 1075.4 (0.41) | 263.9 (0.26) | 261.0 (0.14) | 48.3 | - |
| FA-0.45 | | 464.0 (0.15) | 116.0 (0.04) | - | 1446.5 (0.55) | 261.0 (0.26) | - | - | - |
| FA-IC-0.45 | | 464.0 (0.15) | 116.0 (0.04) | - | 1079.5 (0.41) | 261.0 (0.26) | 258.2 (0.14) | 47.8 | - |
| P-0.35 | 0.35 | 674.2 (0.21) | - | - | 1446.5 (0.55) | 236.0 (0.24) | - | - | 0.75 |
| P-IC-0.35 | | 674.2 (0.21) | - | - | 1019.8 (0.39) | 236.0 (0.24) | 300.1 (0.16) | 55.52 | 0.43 |
| SF-0.35 | | 614.2 (0.20) | - | 49.8 (0.02) | 1446.5 (0.55) | 232.4 (0.23) | - | - | 0.88 |
| SF-IC-0.35 | | 614.2 (0.20) | - | 49.8 (0.02) | 1026.3 (0.39) | 232.4 (0.23) | 295.6 (0.16) | 54.68 | 0.50 |

*Volume fractions

2.3. Curing and conditioning

The samples were demolded after 24 h from casting and then sealed with aluminum tape on all sides but the finished surface to simulate the 1D curing and drying process (Figure 1). Two different external curing methods were implemented for curing the samples (described in Table 3): (1) wet curing with saturated wet burlap for different periods of time and then drying at 50 ± 2 % RH and 23 ± 1 °C (inside an environmental chamber) until the age of 28 days; and (2) curing

compound was applied 30-60 minute after casting and then conditioned inside the environmental chamber until the age of 28 days. The wet curing samples were covered with saturated wet burlap and a plastic sheet for the first 24 h after casting. Two different curing compounds were tested in this study, hydrocarbon resin (CC-Resin) and poly-alpha-methylstyrene (CC-PAMs). The density and volatile organic compound (VOC) level of these curing compounds are given in Table 4. The curing compound was uniformly applied to the surface of the samples using a 3-in paintbrush after bleeding has ceased (30-60 minutes after casting). The samples were weighed before and after the application of the curing compound to calculate the application rate. The application rate was approximately 0.30 ± 0.01 and 0.25 ± 0.02 kg/m² for the CC-Resin and CC-PAMs samples, respectively. This coverage rate was slightly higher than the suggested application rate by the manufacturer (0.20 - 0.22 kg/m²).

Table 3 – External curing practices.

| External Curing Type | Duration | Sample size | Drying condition |
|----------------------|---|--|------------------|
| Wet burlap | 1, 3, 7, 14, and 28 days | 10.2 × 10.2 × 28.0 cm [4x4x11 in.] | 50% RH, 23 °C |
| Curing compound | Apply after 30-60 min and dry until testing | | |

Table 4 – Specifications of the curing compounds used.

| Compounds | ASTM Type | Density (g/cm ³) | Chemistry | VOC (g/L) |
|-----------|-----------------------|---------------------------------|--------------------------|--------------|
| CC-PAMs | Type 2, Class B | 1.03 | poly-alpha-methylstyrene | 297 |
| CC-Resin | Type 1, Classes A & B | 1.01 | water-resin | 278 |

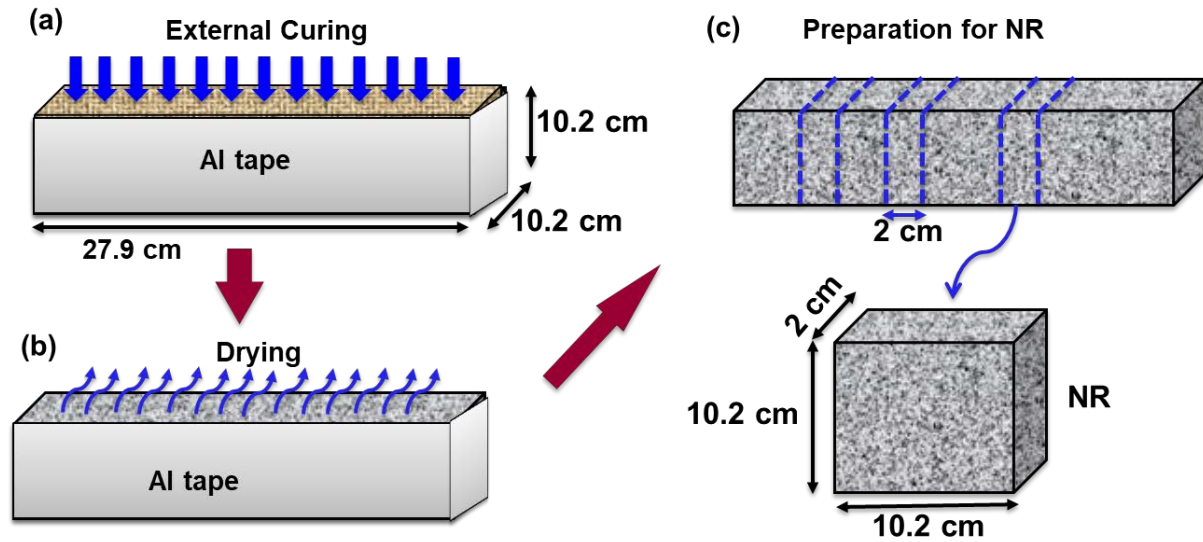


Figure 1 – Schematic representation of (a) wet burlap curing, (b) drying process (conditioning), and (c) preparation of the mortar samples for NR testing.

2.4. Neutron Radiography (NR)

NR was used to determine the volume fraction of chemically bound water (i.e., nonevaporable water) over the depth of all mortar mixtures listed in Table 2, exposed to varying external curing and drying conditions. After the curing and drying period, 20-mm slices (5 per sample) were cut from prismatic samples using a wet saw for the NR experiment (Figure 1). The samples were then dried at 105 ± 2 °C to remove the evaporable water. NR was performed at the Neutron Imaging Facility (NRF) at the Radiation Center in Oregon State University (OSU) (Figure 2). This facility utilizes a 1.1 MW water-cooled research reactor. The beam within the NRF has a collimation ratio (L/D) of 115 ± 4 and a thermal neutron flux of $9.4 \times 10^5 \pm 1.6 \times 10^4$ $\text{cm}^{-2} \text{s}^{-1}$. The NRF is equipped with an image intensifier coupled with a light-tight right angle adapter to a charge-coupled device (CCD) camera as a neutron detection scheme. A Nikon D610 camera with 50 mm f/1.2 lens was used to capture images through the scintillator with a spatial resolution of approximately 90 micrometers. The field of view (FOV) is approximately 150 mm \times 150 mm (39). For each sample, five images were taken with an exposure period of 1 second. A median filter was used to average five images of a sample. Five images of background with open beam (flat-field image) and with closed beam (dark-field image) were also taken. These images were processed using ImageJ software for background correction using dark-field and flat-field images and then analyzed for calculation of the intensity of area of interest in the sample (Figure 2b and c). The attenuation

coefficients of water (0.121 mm^{-1}), oven-dried fine and FLWA aggregates (0.0146 and 0.0155 mm^{-1} respectively), and oven-dried cementitious materials (0.0179 , 0.0130 , and 0.0192 mm^{-1} for OPC, SF, and FA respectively) were also determined using NR.^{25, 33} The following section describes the details of image analysis and non-evaporable water calculation from NR measurements.

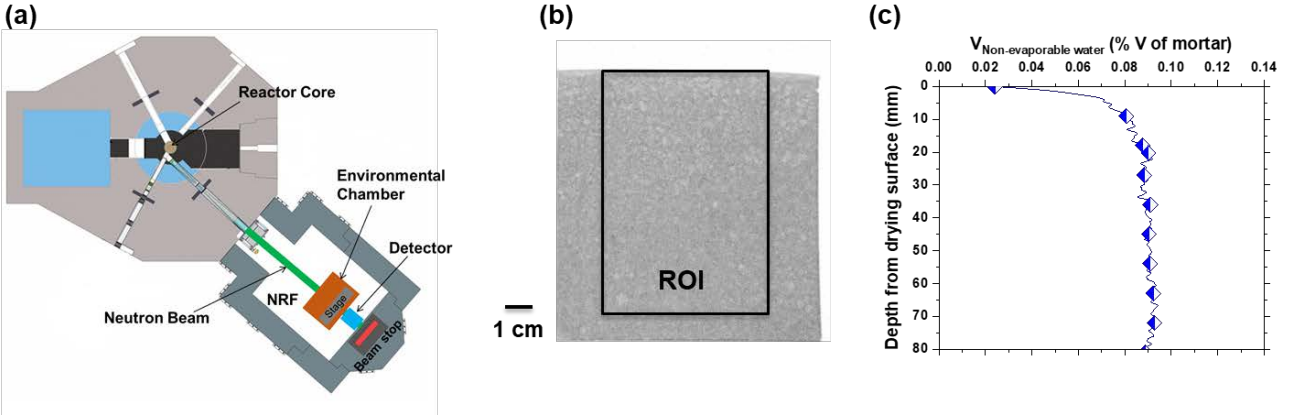


Figure 2 – NR experimental set up: (a) plan view of NRF at OSU (adapted from <https://radiationcenter.oregonstate.edu/oregon-state-triga-reactor-0>) (b) an example of NR image obtained from mortar sample, and (c) an example of analyzed results ($V_{Non-evaporable \text{ water}}$ over depth).

2.5. Determining the non-evaporable water profiles using NR

The images obtained using NR were processed and analyzed using ImageJ software⁴⁰ to determine the volume fraction of non-evaporable water (i.e., chemically bound water). For a mortar system with varying cementitious materials, the Beer-Lambert Law can be re-written to include the contribution of different constituent phases in the hydrated mortar, as shown in Eq. (1).^{25, 26, 28, 32,}

33

$$\ln\left(\frac{I_T}{I_0}\right) = -\mu_s x_s = \sum_{i=1}^n -(\mu_i V_i) x_s = -(\mu_a V_a + \mu_c V_c + \mu_{scm} V_{scm} + \mu_{gs} V_{gs} + \mu_{gw} V_{gw} + \mu_{cw} V_{cw} + \mu_{cs} V_{cs}) x_s \quad (1)$$

where μ_i is the attenuation coefficient of the component ‘ i ’; V_i is the volume fraction of component ‘ i ’; and ‘ i ’ refers to the components aggregate (a), unhydrated cement (c), unreacted SCM (scm), hydrated gel solids (gs), gel water (gw), capillary water (cw), and chemical shrinkage (cs). I_0 and I_T are the intensity of the original beam and the intensity of the beam transmitted through the sample, respectively. x_s is the thickness of the sample. In this formulation, the phase volumes vary

as a function of the degree of hydration and SCM degree of reaction. It should be noted that this formulation does not include entrained or entrapped air however this could be added.

The formulation can be simplified for all the samples in this study as all the evaporable water (chemical shrinkage, gel water, and capillary water) was removed from the system by heating the system to 105 °C (i.e., oven-dried samples). The hydration products consist of gel solids and non-evaporable water which is chemically bound to the gel solids. Gel solids in the plain samples are formed due to cement hydration only, however; in SCM samples the pozzolanic reaction of fly ash or silica fume with calcium hydroxide (CH) leads to the formation of gel solids. Thus, gel solids come from the original volume of cement ($V_{c-original}$), the original volume of SCM ($V_{scm-original}$), and non-evaporable water which is a portion of the original water. It assumed that the volume of the aggregate and cementitious materials do not change during the test (i.e., aggregate and cementitious materials are not lost from the system). Thus, the modified form of Eq. (1) is represented in Eq (2) for the oven-dried systems.^{25, 26, 33}

$$\ln\left(\frac{I_T}{I_0}\right) = -(\mu_a V_a + \mu_c V_{c-original} + \mu_{scm} V_{scm-original} + \mu_w V_{non-evaporable\ water}) x_s \quad (2)$$

Eq. (2) is reordered to determine the volume fraction of non-evaporable water in the mortar from NR as seen in Eq. (3).

$$V_{non-evaporable\ water} = \left[\frac{1}{\mu_w} \right] \left[\frac{\ln\left(\frac{I_0}{I_T}\right)}{x_s} - \mu_a V_a - \mu_c V_{c-original} - \mu_{scm} V_{scm-original} \right] \quad (3)$$

2.6. Thermogravimetric analysis (TGA)

TGA was implemented to investigate the influence of IC on the non-evaporable water content in the core of the samples with and without SCMs. For TGA, a sample was taken from the inner depth (40-60 mm from the exposed surface) of the 20 mm thick slices (Figure 1c). The sample was ground into a fine powder using a laboratory ball mill grinder. Approximately 50 mg of material (6 replicates) was taken from the powdered sample for testing. The powder samples were kept inside a desiccator containing silica gel until testing in order to minimize the carbonation caused by atmospheric CO₂. The analysis was performed by heating the furnace from 23 °C to 1000 °C, at a rate of 20 °C/minute in a nitrogen-purged atmosphere.

The amount of non-evaporable water was estimated by analyzing TGA and derivative thermogravimetry (DTG) curves using the modified tangential method (calculated as the difference between the 105 °C and 580 °C, and 746 °C and 1000 °C mass loss measurements to account for the loss on ignition (LOI) of the cementitious materials and the aggregates). The mixture proportions from Table 2 were used to calculate the volume fraction of non-evaporable water.

3. Results and Discussion

3.1. Non-evaporable water profiles

The volume fraction of non-evaporable water (i.e., chemically bound water) in mortar samples is related to the volume fraction of hydration products (i.e., degree of hydration of cement) and pozzolanic reaction products (i.e., degree of reaction of SCM).^{21, 25, 41} As detailed in section 2, NR images can be used to determine the volume fraction of non-evaporable water with a high spatial resolution (≈ 90 micrometers) over depth (Eq. 3). The volume fraction of non-evaporable water profiles for mixtures with w/cm of 0.45 and 0.35 with varying wet burlap curing duration are shown in Figures 3 and 4, respectively.

Based on the results, wet curing with saturated burlap showed a significant improvement in $V_{Non-evaporable\ water}$ at the top 20 mm of the sample surface by extending the wet curing duration. The average $V_{Non-evaporable\ water}$ increased about 10-40% in 20 mm of the surface of the OPC and FA samples by extending the wet burlap duration from 1 to 7 days. The IC samples showed a 10-20% increase in the average $V_{Non-evaporable\ water}$ at the top 20 mm (i.e., cover) of the sample compared to virgin mixtures. In addition, the IC samples had 5-15% greater $V_{Non-evaporable\ water}$ at the core than the virgin samples.

The $V_{Non-evaporable\ water}$ in the core of the OPC system (w/cm=0.45) is about 8-15% greater than that of the FA mixtures (w/cm=0.45). The OPC system with a w/cm of 0.35 showed higher $V_{Non-evaporable\ water}$ in the surface and core of the sample compared to the OPC samples with a w/cm of 0.45. This increase in non-evaporable water is due, in part, to the higher cement content in the mortar mixtures with a w/cm of 0.35. The SF samples showed a reduction in $V_{Non-evaporable\ water}$ when compared to the OPC samples. These results from NR are in agreement with the results of TGA, as shown in

Figure 5. Based on Figure 5, the IC samples showed about 4-15% greater $V_{Non-evaporable\ water}$ in the core of the samples when compared to the conventional mixtures without IC.

A comparison between the results of FA samples with curing compound and wet burlap curing regimes is shown in Figure 6. The application of CC-PAMs increased the $V_{Non-evaporable\ water}$ in the cover of the sample (first 20 mm from the surface) compared to 1-day wet burlap cured samples, and the CC-PAMs samples showed a similar performance to the 7-day wet burlap cured samples. However, the CC-Resin was not as effective in retaining the water inside the system and had lower $V_{Non-evaporable\ water}$ in the first 20 mm from the surface when compared to the CC-PAMs and 7-day wet burlap cured samples. The improved performance by the CC-PAMs (a solvent-based curing compound) can be attributed to more uniform coverage due to the improvements in wetting provided by solvents when compared to water-based curing compounds (CC-Resin).⁵ Additionally, it is suggested that solvent-based curing compounds have less vapor permeability than water-based curing compounds.⁴²

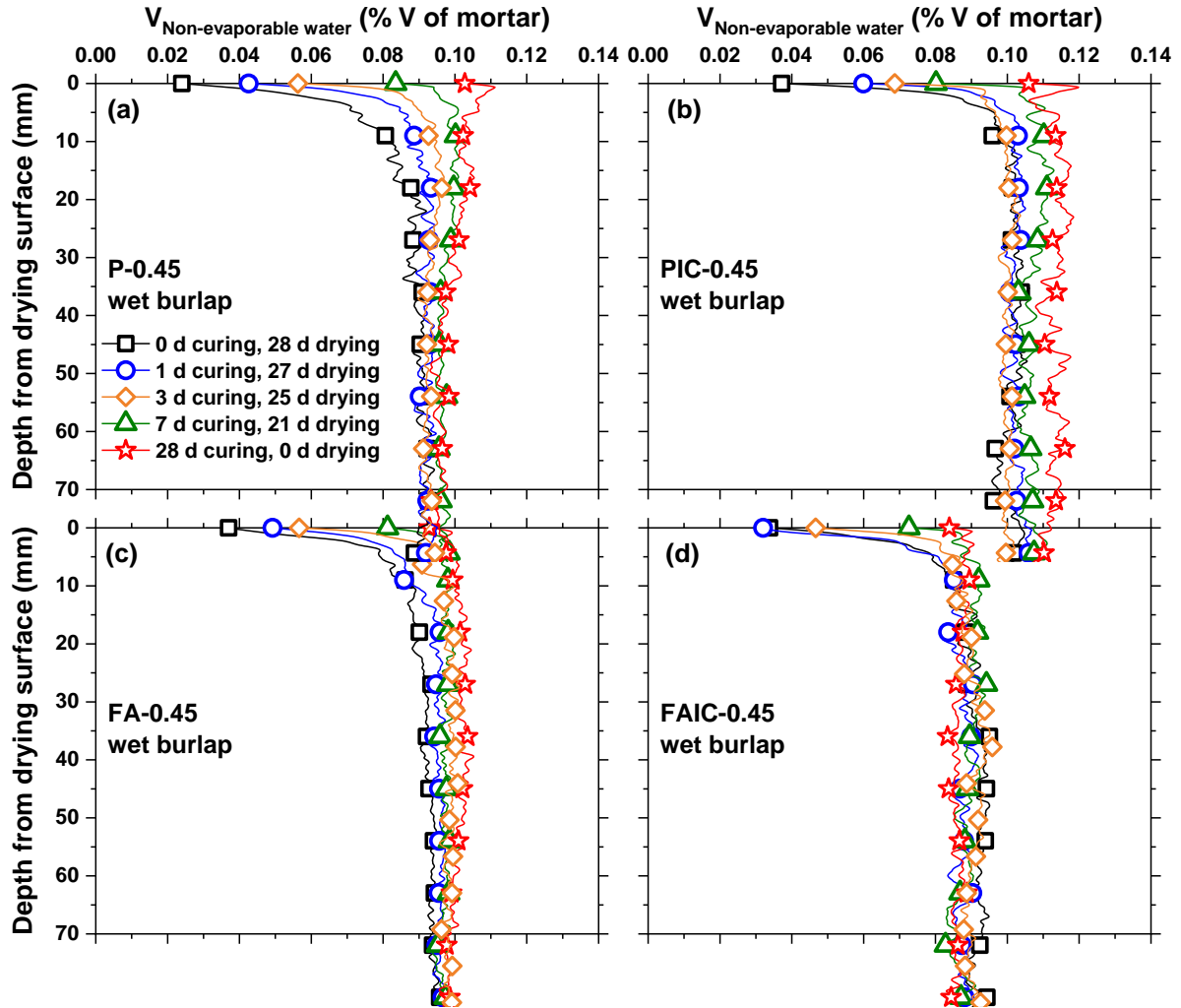


Figure 3 – Profiles of volume fraction of non-evaporable water over depth for OPC and FA mortar samples ($w/cm=0.45$) with varying wet burlap curing durations: (a) P-0.45, (b) PIC-0.45, (c) FA-0.45, and (d) FAIC-0.45.

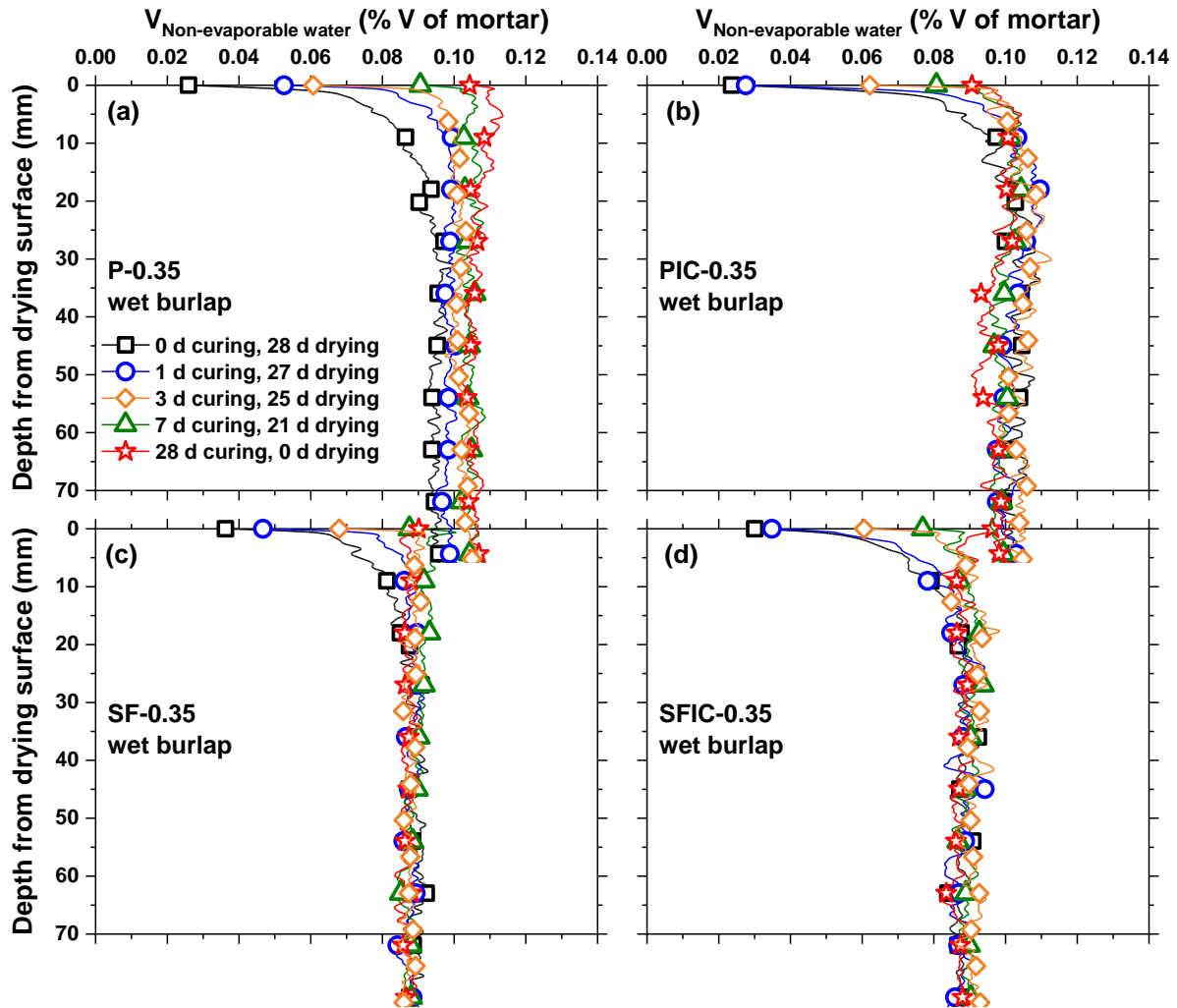


Figure 4 – Profiles of volume fraction of non-evaporable water over depth for OPC and SF mortar samples ($w/cm=0.35$) with varying wet burlap curing durations: (a) P-0.35, (b) PIC-0.35, (c) SF-0.35, and (d) SFIC-0.35.

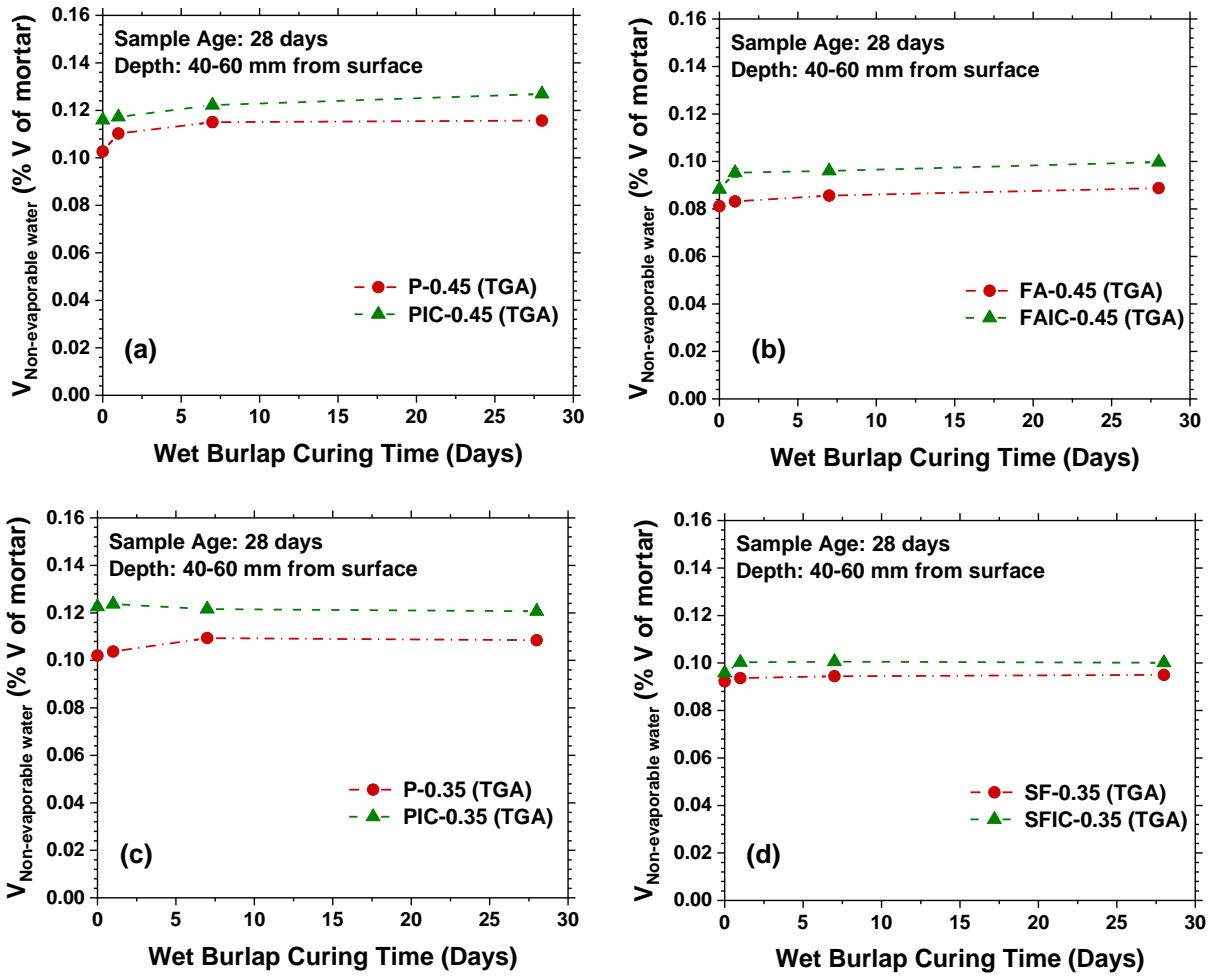


Figure 5 – The $V_{Non-evaporable\ water}$ in the core of the samples (40-60 mm from the exposed surface) as a function of wet burlap curing time for different mortar mixtures with and without IC (by TGA): (a) OPC-w/cm=0.45, (b) FA-w/cm=0.45, (c) OPC-w/cm=0.35, and (d) SF-w/cm=0.35.

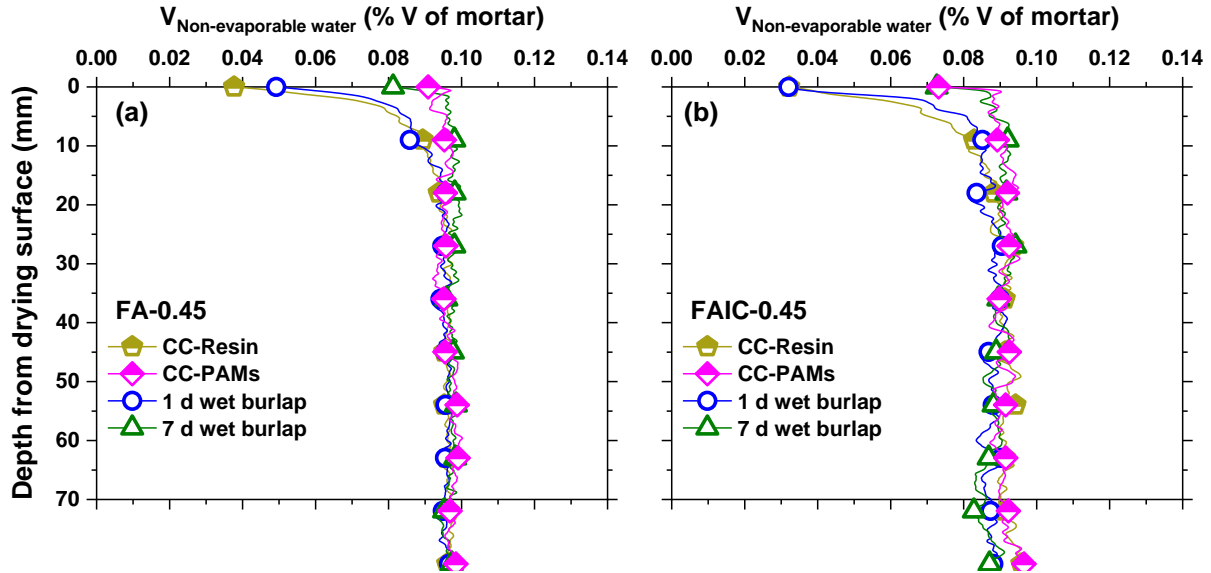


Figure 6 – Comparison between $V_{Non-evaporable\ water}$ profiles for FA mortar samples ($w/cm=0.45$) with CC-Resin and CC-PAMs curing compounds and 1-day and 7-day wet burlap cured samples: (a) FA-0.45 and (b) FAIC-0.45.

3.2. Determining the curing-affected zone (CAZ) as a function of curing time

While the entire cross-section of concrete requires curing, the surface of the concrete is the most sensitive to moisture loss, and therefore is the most sensitive to curing methods.¹⁶ Cather¹⁶ defined this zone at the surface of the concrete as the curing-affected zone (CAZ) and a thinner CAZ in aged concrete indicates curing measures were more effective. While defining the CAZ is difficult, this study implements the non-evaporable water profiles from NR to quantify the CAZ with a high spatial resolution for different curing practices.

Figure 7 shows an example of the CAZ measurement. The CAZ was defined as a distance that extends from the surface of the sample to a depth that the non-evaporable water profile intersects with the average non-evaporable water content line.²⁵ The average non-evaporable water content was calculated as the depths of the sample where the coefficient of variation (COV) of data is less than 2.0%. Additionally, the intersection point was selected in order that it is not within one standard deviation of the average line.

The measured CAZ values for different mixtures with and without IC are illustrated in Figure 8. The CAZ value decreases by extending the wet curing duration in both OPC and SCM systems (it approaches zero after 14 days of wet curing). The FA samples with no external curing had the

largest CAZ (26 mm and 15 mm for the samples with and without IC respectively (Figure 8b). This is attributed to the increased evaporation at the surface (as can be seen in Figure 3). The application of IC mixtures considerably lower the CAZ value, especially in the samples with limited external curing duration (up to ≈ 15 mm reduction in CAZ value). As expected, the samples with a low w/cm showed a reduction in CAZ values as illustrated in Figures 8c and d. As shown in Figure 9, the application of CC-PAMs considerably reduced the CAZ value (< 1 mm), while the FA sample with CC-Resin showed a 16 mm of CAZ (similar to that of 1-day wet burlap cured sample).

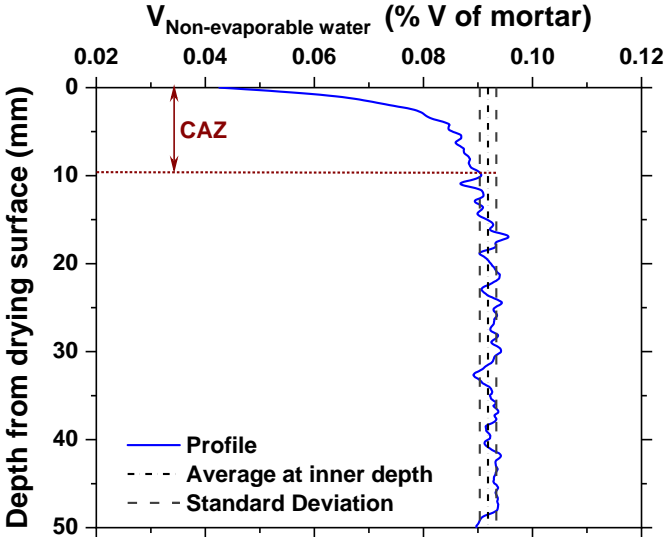


Figure 7 – Determination of the CAZ using the non-evaporable water profile by NR.

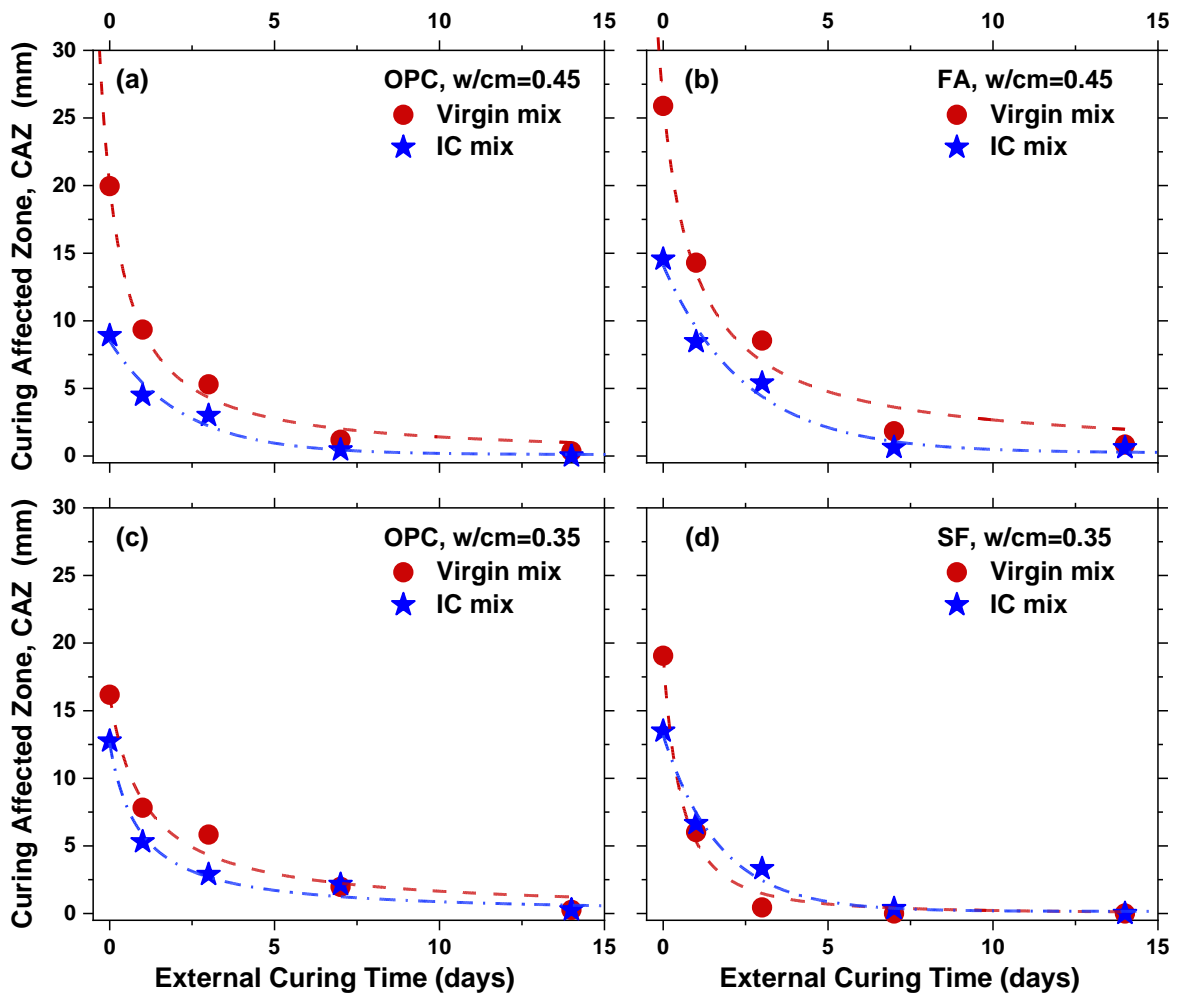


Figure 8 – CAZ as a function of wet burlap curing time for different mortar mixtures with and without IC:
 (a) OPC-w/cm=0.45, (b) FA-w/cm=0.45, (c) OPC-w/cm=0.35, and (d) SF-w/cm=0.35.

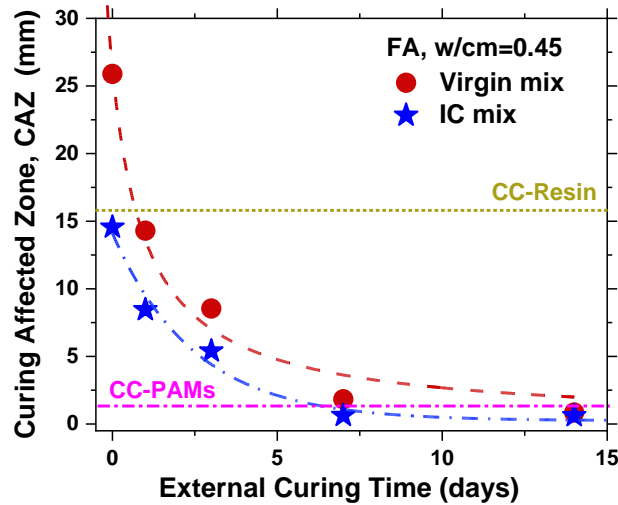


Figure 9 – Comparison of CAZ for FA samples ($w/cm=0.45$) with curing compound and wet burlap curing methods.

3.3. Establishing ‘Equivalency Lines’

One approach that can be used to evaluate the efficiency of curing is to determine the duration of curing required to provide equivalent performance. Here equivalent performance is defined by the depth of the CAZ. Figure 10a shows an example of how this approach can be applied to virgin and IC samples exposed to wet burlap curing. For a CAZ that is 2.5 mm, the plain mixture required 5 days of wet burlap curing while the IC mixture required 2.5 days of wet burlap curing. The time of equivalent curing was determined for other depths (i.e., the difference between the fitted curves), as shown in Figure 10b. The curing time needed for a given curing technology (IC in this case) is the slope of the equivalency line. For example, IC mixtures require 0.414 the time required for the control mixture.

Figure 11 illustrates the equivalency approach for the OPC and SCM mixtures with w/cm of 0.35 and 0.45. As shown in Figure 11a, the slope of the equivalency lines for the OPC and FA mixtures ($w/cm=0.45$) is 41.4% and 46.3%, respectively. This shows that the application of IC in OPC and FA mixtures ($w/cm=0.45$) reduced the duration of external curing by 58.6% and 53.7%, respectively. The reduction in curing time was slightly less effective in the w/cm of 0.35 (Figure 11b).

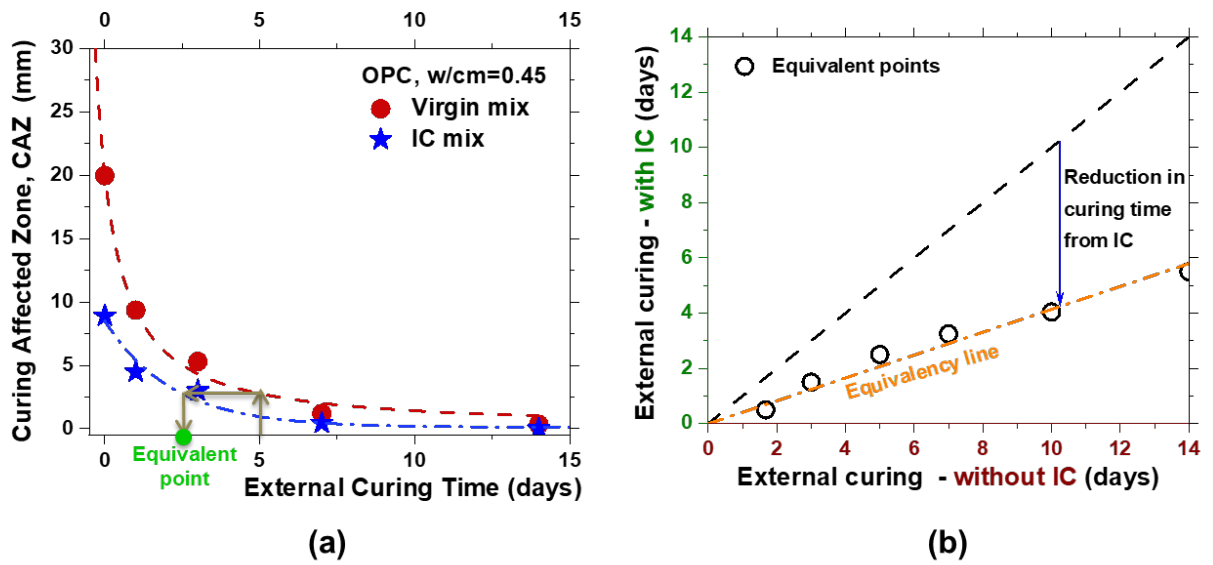


Figure 10 – (a) Determination of equivalent points between the virgin and IC mixtures using CAZ profiles (difference between the fitted curves) and (b) an example of the correlation between the use of IC and equivalent external curing durations (i.e., equivalency line using CAZ).

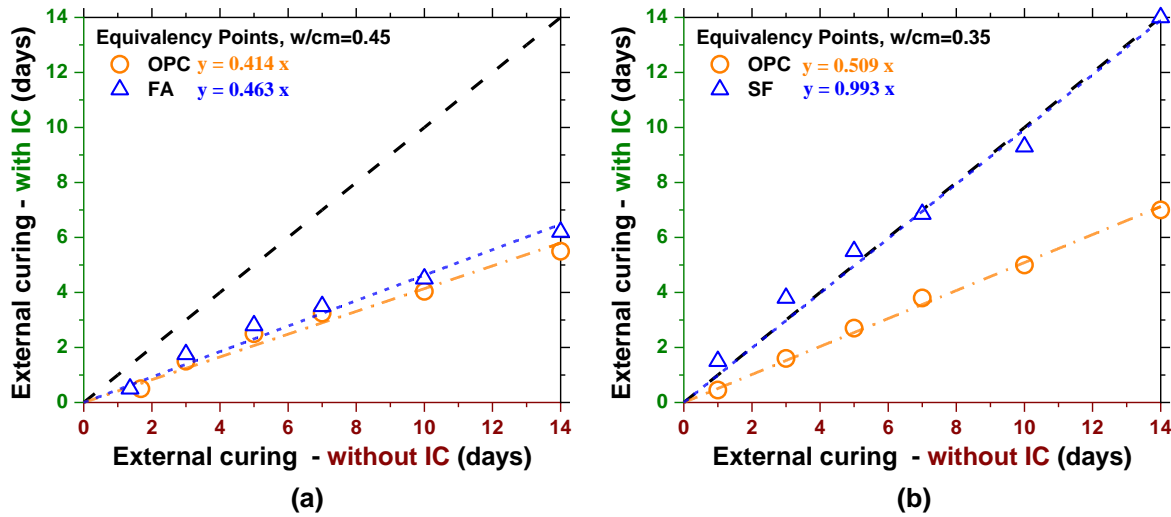


Figure 11 – Correlation between the use of IC and equivalent external curing durations (i.e., equivalency line using CAZ): (a) OPC and FA mixtures (w/cm=0.45) and (b) OPC and SF mixtures (w/cm=0.35).

3.4. Practical implications

The benefits of various curing technologies have been determined using neutron radiography which provides spatial resolution and the ability to determine the content of non-evaporable water. This approach enables the CAZ to be determined with a high degree of precision. The CAZ can be used to develop quantifiable equivalent durations of curing when different curing technologies are used. This provides the potential for equivalent performance criteria to be developed that can be incorporated into curing guidelines and specifications. This approach could enable the concrete industry to better quantify and specify curing based on performance, which provides an effective methodology for establishing new curing guidelines.

IC mixtures show a thinner CAZ than conventional mixtures except for the silica fume mixture. More work is needed to further understand this behavior of silica fume samples. However, it should be noted that the silica fume samples with IC showed about 8% greater $V_{Non-evaporable\ water}$ in the core of the samples compared to the samples without IC. As such, when CAZ is used to obtain equivalent performance, the duration of external curing could be reduced by 49.1 to 58.6 % with 53.8% being the average benefit. The experiments were performed using a small number of materials and curing conditions in this study. The results suggest that IC may provide contractors with an alternative curing practice when construction schedules are accelerated. It is worth noting that further study is needed to obtain the equivalent performance of IC mixtures using other performance criteria such as surface hardness, abrasion resistance, scaling resistance, and surface permeability.

4. Conclusions

This study investigated the efficiency of different curing practices using neutron radiography. Eight different mortar mixtures were examined with two different w/cm (0.35 and 0.45) with and without SCMs. Neutron radiography (NR) was used to determine the non-evaporable water content in different systems as a function of depth. This information was used to quantify the curing-affected zone (CAZ), and the CAZ was used to develop equivalent durations of curing for concrete with conventional external curing and internal curing.

Wet curing with saturated burlap showed an improvement with longer curing duration (as measured by non-evaporable water), as one would expect. The application of poly-alpha-methylstyrene based curing compounds (CC-PAMs) in FA mixtures increased the volume fraction of non-evaporable water in the top 20 mm of the sample, however, the hydrocarbon resin (CC-Resin) did not demonstrate a significantly different behavior than 1-day wet burlap curing. The application of CC-PAMs considerably reduced the CAZ value (< 1 mm), while the FA sample with CC-Resin showed a 16 mm of CAZ.

In general, IC samples showed an increase of 10-20% in the non-evaporable water content at the surface of the samples and 5-15% at the core as compared to the plain concrete mixture. The application of internally cured mixtures considerably lowered the CAZ thickness, especially in the samples with limited external curing duration (up to 15 mm [0.6 in.]).

Equivalent performance is defined by the depth of the CAZ in this study. IC mixtures with w/cm of 0.45 reduced the duration of external curing by 50-60%. This would imply that, for cases where 14-days of wet burlap may be specified on a bridge deck, 7 days of wet burlap with internal curing can provide the same level of curing performance (using CAZ as the measure). The reduction in duration of external curing by use of IC is smaller in the silica fume mixtures.

5. References

1. American Concrete Institute, "ACI PRC-308-16 Guide to External Curing of Concrete," ACI Committee 308, Farmington Hills, Michigan, USA, 2016, pp. 36.
2. Kosmatka SH, Kerkhoff B, Panarese WC, "Design and control of concrete mixtures." Portland Cement Association, Skokie, IL; 2018.
3. Taylor PC, "Curing concrete." CRC Press; 2013.
4. Carrier RE, Cady P, "Evaluating effectiveness of concrete curing compounds," Journal of materials. V. 5, No. 2, 1970, pp. 294-302.
5. Hajibabae A, Khanzadeh Moradllo M, Ley MT, "Comparison of curing compounds to reduce volume change from differential drying in concrete pavement," International Journal of Pavement Engineering, V. 19, No. 9. 2018, pp. 815-24.
6. Bentz DP, Weiss WJ, "Internal curing: a 2010 state-of-the-art review." US Department of Commerce, National Institute of Standards and Technology; 2011.
7. Henkensiefken R, Nantung T, Weiss J, "Saturated lightweight Aggregate for internal curing in low w/c mixtures: monitoring water movement using X-ray absorption," Strain, V. 47. 2011, pp. e432-e41.
8. Kevern JT, Nowasell QC, "Internal curing of pervious concrete using lightweight aggregates," Construction and Building Materials, V. 161. 2018, pp. 229-35.
9. Kovler K, Jensen O, "Internal curing of concrete: State-of-the-Art Report. of RILEM Technical Committee," 196-ICC, 2007.
10. Schroefl C, Mechtcherine V, Vontobel P, Hovind J, Lehmann E, "Sorption kinetics of superabsorbent polymers (SAPs) in fresh Portland cement-based pastes visualized and quantified by neutron radiography and correlated to the progress of cement hydration," Cement and Concrete Research, V. 75. 2015, pp. 1-13.
11. Weiss WJ, Morian D, "Review of Internally Cured Concrete as It Relates to Pavements," Transportation Research Board 96th Annual Meeting, Washington, DC, USA, 2017, pp.
12. Barrett TJ, Miller AE, Weiss WJ, "Documentation of the INDOT experience and construction of the bridge decks containing internal curing in 2013," Purdue University. Joint Transportation Research Program, 2015, pp. 15.
13. Rupnow T, "Lightweight Aggregate and Internally Cured Concrete (ICC) Prove Their Value on Louisiana Bridge," Louisiana DOT, 2015.
14. Weiss WJ, Montanari L, "Guide Specification for Internally Curing Concrete," InTrans Project 13-482, National Concrete Pavement Technology Center, Ames, IA, USA, 2017.

15. Huebschman CR, Garcia C, Bullock DM, Abraham DM, "Construction work zone safety." FHWA/IN/JTRP-2002/34. Joint Transportation Research Program, Indiana Department of Transportation and Purdue University, West Lafayette, Indiana, 2003.
16. Cather B, "How to get better curing," *Concrete (London)*, V. 26, No. 5. 1992, pp. 22-5.
17. Dhir R, Hewlett P, Chan Y, "Near-surface characteristics of concrete: abrasion resistance," *Materials and Structures*, V. 24, No. 2. 1991, pp. 122-8.
18. Hajibabae A, Moradllo MK, Behravan A, Ley MT, "Quantitative measurements of curing methods for concrete bridge decks," *Construction and Building Materials*, V. 162. 2018, pp. 306-13.
19. Jensen OM, Hansen PF, "Autogenous relative humidity change in silica fume-modified cement paste," *Advances in Cement Research*, V. 7, No. 25. 1995, pp. 33-8.
20. Poole TS, "Guide for Curing of Portland Cement Concrete Pavements, Volume I," FHWA-RD-02-099, USAE Research and Development Center (ERDC), Structures Laboratory, Vicksburg, MS, USA, 2005.
21. Powers TC, "Structure and physical properties of hardened Portland cement paste," *Journal of the American Ceramic Society*, V. 41, No. 1. 1958, pp. 1-6.
22. Villani C, "Transport processes in partially saturate concrete: Testing and liquid properties," PhD Thesis, Purdue University, West Lafayette, IN, USA, 2014.
23. Hanson J, "Effects of curing and drying environments on splitting tensile strength of concrete," *Journal Proceedings*, V. 65, No. 7, 1968, pp. 535-43.
24. Khanzadeh-Moradllo M, Meshkini MH, Eslamdoost E, Sadati S, Shekarchi M, "Effect of wet curing duration on long-term performance of concrete in tidal zone of marine environment," *International Journal of Concrete Structures and Materials*, V. 9, No. 4. 2015, pp. 487-98.
25. Khanzadeh Moradllo M, Montanari L, Suraneni P, Reese SR, Weiss J, "Examining curing efficiency using neutron radiography," *Transportation Research Record*, V. 2672, No. 27. 2018, pp. 13-23.
26. Choudhary A, Khanzadeh Moradllo, M., Reese, S. R., Weiss, W. J., "Examining curing efficiency in fly ash concrete using neutron radiography," *ACI-ICI*, India, 2018.
27. Berger H, "Neutron radiography," *Annual Review of Nuclear Science*, V. 21, No. 1. 1971, pp. 335-64.
28. Hussey DS, Spornjak D, Weber AZ, Mukundan R, Fairweather J, Brosha EL, et al., "Accurate measurement of the through-plane water content of proton-exchange membranes using neutron radiography," *Journal of Applied Physics*, V. 112, No. 10. 2012, pp. 104906.
29. Sears VF, "Neutron scattering lengths and cross sections," *Neutron news*, V. 3, No. 3. 1992, pp. 26-37.

30. De Beer F, Strydom W, Griesel E, "The drying process of concrete: a neutron radiography study," *Applied Radiation and Isotopes*, V. 61, No. 4. 2004, pp. 617-23.
31. Kanematsu M, Maruyama I, Noguchi T, Iikura H, Tsuchiya N, "Quantification of water penetration into concrete through cracks by neutron radiography," *Nuclear Instruments and Methods in Physics Research Section A: Accelerators, Spectrometers, Detectors and Associated Equipment*, V. 605, No. 1-2. 2009, pp. 154-8.
32. Lucero CL, Bentz DP, Hussey DS, Jacobson DL, Weiss WJ, "Using neutron radiography to quantify water transport and the degree of saturation in entrained air cement based mortar," *Physics Procedia*, V. 69. 2015, pp. 542-50.
33. Khanzadeh Moradillo M, Chung C-W, Keys MH, Choudhary A, Reese SR, Weiss WJ, "Use of borosilicate glass powder in cementitious materials: Pozzolanic reactivity and neutron shielding properties," *Cement and Concrete Composites*, V. 112. 2020, pp. 103640.
34. Khanzadeh Moradillo M, Qiao C, Keys M, Hall H, Ley M, Reese S, et al., "Quantifying fluid absorption in air-entrained concrete using neutron radiography," *ACI Materials Journal*, V. 116, No. 6. 2019, pp. 213-26.
35. Najjar WS, Aderhold HC, Hover KC, "The application of neutron radiography to the study of microcracking in concrete," *Cement, concrete and aggregates*, V. 8, No. 2. 1986, pp. 103-9.
36. Trtik P, Münch B, Weiss WJ, Kaestner A, Jerjen I, Josic L, et al., "Release of internal curing water from lightweight aggregates in cement paste investigated by neutron and X-ray tomography," *Nuclear Instruments and Methods in Physics Research Section A: Accelerators, Spectrometers, Detectors and Associated Equipment*, V. 651, No. 1. 2011, pp. 244-9.
37. Villani C, Lucero C, Bentz D, Hussey D, Jacobson DL, Weiss W, "Neutron radiography evaluation of drying in mortars with and without shrinkage reducing admixtures," *ACI Proceedings*, 26, 2014.
38. Zhang P, Wittmann FH, Zhao T-j, Lehmann EH, Vontobel P, "Neutron radiography, a powerful method to determine time-dependent moisture distributions in concrete," *Nuclear Engineering and Design*, V. 241, No. 12. 2011, pp. 4758-66.
39. Khanzadeh Moradillo M, Reese SR, Weiss WJ, "Using neutron radiography to quantify the settlement of fresh concrete," *Advances in Civil Engineering Materials*, V. 8, No. 1. 2019, pp. 71-87.
40. Schneider CA, Rasband WS, Eliceiri KW, "NIH Image to ImageJ: 25 years of image analysis," *Nature methods*, V. 9, No. 7. 2012, pp. 671-5.
41. Fagerlund G, "Chemically bound water as measure of degree of hydration: method and potential errors." (Report TVBM; Vol. 3150). Division of Building Materials, LTH, Lund University, 2009.

42. Dhir R, Levitt M, Wang J, "Membrane curing of concrete: water vapour permeability of curing membranes," Magazine of Concrete Research, V. 41, No. 149. 1989, pp. 221-8.

Appendix: TechNote Outline

A proposal for TechNote was submitted to the ACI Committee 213 in May 2021 in order to lead the TechNote development and obtain TAC approval. The outline of TechNote is provided in the following. Upon receiving approval, the TechNote will be shared with ACI committees 213 for review, voting, and submission to TAC.

Why this TechNote is needed?

Curing is important to develop long-lasting durable concrete. Curing promotes hydration of the cement and reaction of the supplementary cementitious materials (SCMs) leading to improved strength and durability. Concrete specifications typically specify curing as a fixed duration of time (e.g., 14 days of curing using wet burlap). Currently, State Highway Agencies (SHA) are actively seeking ways in which they can reduce the time of construction to reduce the inconvenience to the traveling public and to improve safety for the construction workers in work zones. As such, it is often asked if the specified duration of curing can be reduced, especially by implementing new curing practices such as internal curing. However, relatively limited literature has been published to understand how the benefits of internal curing practices can be achieved in the construction process. Based on the findings of ongoing research (sponsored by the ACI Foundation), this TechNote will present quantifiable equivalent durations of curing for concrete with conventional curing and internal curing using pre-wetted fine lightweight aggregates in OPC and SCM systems. It is shown that the use of internally cured concrete mixtures can reduce curing time saving contractors both time and money during construction. For example, while a 14-day wet burlap may be specified on a bridge deck, it may be possible that 7 days of wet burlap with internal curing provides the same level of performance. This would reduce the construction schedule by one week. This TechNote will provide tools to enable practitioners to implement internal curing for different applications due to its advantages in saving both time and money during construction.

Preliminary Outline

Document No. XXX

TechNote

CURING EFFICIENCY OF INTERNALLY CURED CONCRETE

Keywords: internal curing; lightweight aggregates; curing duration; degree of hydration; wet burlap curing; curing compound; supplementary cementitious materials

Introduction

This section will discuss the significance and objectives of this TechNote.

Question

How does the internal curing impact the duration of curing to have equivalent performance to conventional externally cured concrete?

Answer

Based on the findings of this research (sponsored by the ACI Foundation), this section will provide a brief answer to the above question.

Discussion

A detailed discussion on the impact of internally cured concrete on the duration of curing in OPC and SCM mixtures will be provided in this section. This will include details on examined mixtures, curing and conditioning practices, and conducted experiments.

Equivalency Equations

This subsection will specify the correlation between the use of internal curing and equivalent external curing durations for different mixtures. A Table summarizing the results will be provided.

Practical Implication

The potential implementation of the findings in practice will be discussed in this subsection.

Summary

The summary will include the main objective and implication of this TechNote.

References

References will be listed according to the ACI format.